The Astrophysical Journal, 948:123 (11pp), 2023 May 10 https://doi.org/10.3847/1538-4357/acb698

On the Hunt for the Origins of the Orphan–Chenab Stream: Detailed Element Abundances with APOGEE and Gaia

Keith Hawkins[1], Adrian M. Price-Whelan[2], Allyson A. Sheffield[3], Aidan Z. Subrahimovic[4], Rachael L. Beaton[5], Vasily Belokurov[2,6], Denis Erkal[7], Sergey E. Koposov[8,9], Richard R. Lane[10], Chervin F. P. Laporte[11], and Christian Nitschelm[12]

[1] Department of Astronomy, The University of Texas at Austin, 2515 Speedway Boulevard, Austin, TX 78712, USA; keithhawkins@uteaxs.edu
[2] Center for Computational Astrophysics, Flatiron Institute, 162 Fifth Avenue, New York, NY 10010, USA
[3] CUNY—LaGuardia Community College, Department of Natural Sciences, Long Island City, NY 11101, USA
[4] Center for Cosmology and Particle Physics, New York University, Department of Physics, 726 Broadway, New York, NY 10003, USA
[5] The Observatories of the Carnegie Institution for Science, 813 Santa Barbara Street, Pasadena, CA 91101, USA
[6] Institute of Astronomy, Madingley Rd, Cambridge, CB3 0HA, UK
[7] Department of Physics, University of Surrey, Guildford, GU2 7XH, UK
[8] Institute for Astronomy, University of Edinburgh, Royal Observatory, Blackford Hill, Edinburgh, EH9 3HJ, UK
[9] Institute of Astronomy, University of Cambridge, Madingley Road, Cambridge, CB3 0HA, UK
[10] Centro de Investigación en Astronomía, Universidad Bernardo O'Higgins, Avenida Viel 1497, Santiago, Chile
[11] Institut de Ciencies del Cosmos (ICCUB), Universitat de Barcelona (IEEC-UB), Martí Franqués 1, E-08028 Barcelona, Spain
[12] Centro de Astronomía (CITEVA), Universidad de Antofagasta, Avenida Angamos 601, Antofagasta 1270300, Chile
Received 2022 May 27; revised 2023 January 17; accepted 2023 January 18; published 2023 May 15

Abstract

Stellar streams in the Galactic halo are useful probes of the assembly of galaxies like the Milky Way. Many tidal stellar streams that have been found in recent years are accompanied by a known progenitor globular cluster or dwarf galaxy. However, the Orphan–Chenab (OC) stream is one case where a relatively narrow stream of stars has been found without a known progenitor. In an effort to find the parent of the OC stream, we use astrometry from the early third data release of ESA's Gaia mission (Gaia EDR3) and radial velocity information from the Sloan Digital Sky Survey (SDSS)-IV Apache Point Observatory Galactic Evolution Experiment (APOGEE) survey to find up to 13 stars that are likely members of the OC stream. We use the APOGEE survey to study the chemical nature (for up to 10 stars) of the OC stream in the α (O, Mg, Ca, Si, Ti, and S), odd-Z (Al, K, and V), Fe-peak (Fe, Ni, Mn, Co, and Cr), and neutron-capture (Ce) elemental groups. We find that the stars that make up the OC stream are not consistent with a monometallic population and have a median metallicity of -1.92 dex with a dispersion of 0.28 dex. Our results also indicate that the α elements are depleted compared to the known Milky Way populations and that its [Mg/Al] abundance ratio is not consistent with second-generation stars from globular clusters. The detailed chemical pattern of these stars, namely the [α/Fe]–[Fe/H] plane and the metallicity distribution, indicates that the OC stream progenitor is very likely to be a dwarf spheroidal galaxy with a mass of $\sim 10^6\,M_\odot$.

Unified Astronomy Thesaurus concepts: Stellar streams (2166); Chemical abundances (224); Stellar abundances (1577)

1. Introduction

In ΛCDM cosmology, it is believed that galaxies in general are assembled in a hierarchical way through the accretion of small sub-Galactic systems to construct larger ones and eventually systems over broad ranges in mass and size (e.g., Searle & Zinn 1978; Davis et al. 1985; Bullock & Johnston 2005). In this context, one would expect the stellar halo of the Milky Way to be built largely from the accretion of smaller objects, as well as a smaller component of material formed within its viral radius (so-called in situ material, e.g., Helmi & de Zeeuw 2000; Cooper et al. 2015; Hawkins et al. 2015; Bonaca et al. 2017, and references therein).

The Galactic halo contains many relic substructures in the form of gravitationally bound clusters and dwarf galaxies and disrupted analogs in the form of tidal stellar streams from both globular clusters and dwarf galaxies alike. The modern "field of streams" (Belokurov et al. 2006; Bonaca et al. 2012) in our stellar halo demonstrates the importance of accretion processes in the build up of stellar halos. Studying the amount and properties of substructure in the Milky Way's stellar halo has provided an important way of constraining the importance of accretion processes in forming stellar halos (e.g., Naidu et al. 2020), of measuring the mass and profile of DM in the galaxy (e.g., Majewski et al. 2003; Koposov et al. 2010; Law & Majewski 2010; Gibbons et al. 2014), and of constraining the small-scale properties of DM within galaxies (e.g., Carlberg et al. 2012; Erkal et al. 2016; Price-Whelan & Bonaca 2018; Bonaca et al. 2019; Banik et al. 2021).

In this work, we focus on the Orphan–Chenab (OC) Stream: the Orphan stream was discovered independently by two separate teams (Grillmair 2006; Belokurov et al. 2007) and the Chenab Stream was discovered photometrically as a roughly 19° stellar feature in the Dark Energy Survey DR1 (Shipp et al. 2018), in the same direction on the sky as the southern Galactic component of the Orphan Stream and at an estimated photometric distance of 40 kpc. The spatial overlap between the Orphan and Chenab streams was shown in the all-sky view presented by Koposov et al. (2019). Additionally, both Koposov et al. (2019) and Shipp et al. (2019) illustrated that

the proper motion signals of the Orphan and Chenab streams are consistent. The equivalence of the Orphan and Chenab streams across multiple kinematic parameters is now understood as strong evidence that these streams are both remnants of the tidal disruption of the same progenitor. In particular, a misalignment in the northern/southern stream poles can be explained by a dynamic encounter of the southern portion of the OC stream with the Large Magellanic Cloud (Erkal et al. 2019).

Despite being a large structure traced over $\sim 210^\circ$ on the sky (or $\sim$150 kpc in physical length; Grillmair et al. 2015; Fardal et al. 2019; Koposov et al. 2019), the OC stream still has no known progenitor system. The OC stream is also relatively narrow, just $\sim 2^\circ$ wide on the sky, but its width is significantly broader than known streams associated with globular cluster systems (e.g., the Palomar 5 stream; Odenkirchen et al. 2003; Erkal et al. 2017; Bonaca et al. 2020). However, the stellar mass of the OC stream implies that the system that it originated in could be on the massive end of classical globular clusters (e.g., Grillmair 2006; Belokurov et al. 2007). The stream is also relatively low in surface brightness and has a distance range from $\sim$19 to 55 kpc (there is a steep distance gradient along the stream; Sesar et al. 2013; Koposov et al. 2019). Recent orbital fitting of the stream indicates that it has a Galactocentric pericenter of $\sim$16 kpc and an apocenter of $\sim$90 kpc (e.g., Newberg et al. 2010), which implies a very eccentric orbit.

There are several theories for the potential progenitors to the OC stream. The first is that the OC stream originates from a globular cluster system. Koposov et al. (2019) has found that as many as seven globular clusters are within 7° of the stream's great circle (see the top panel of their Figure 14). Of these globular clusters, two have been discussed in the literature as potential parents for the Orphan stream, namely NGC 2419 (discussed in Brüns & Kroupa 2011) and Ruprecht 106 (discussed in Grillmair et al. 2015; Koposov et al. 2019). However, both are thought implausible based on chemokinematic arguments (e.g., Casey et al. 2014; Grillmair et al. 2015). Recently, Li et al. (2022) noted that the globular cluster system Laevens 3 (Laevens et al. 2015), may be a potential progenitor of the OC stream. The chemical exploration of the OC stream in this study will enable us to test this idea further. Another possibility is that the OC stream has originated from an ultrafaint dwarf galaxy, such as Segue 1 (e.g., Gilmore et al. 2013; Casey et al. 2014), Ursa Major II (e.g., Fellhauer et al. 2007), or Grus II (e.g., Koposov et al. 2019). Distinguishing between these theories of the long lost parent of the OC stream is, in some sense, the great challenge. The kinematic, spatial, and chemical nature of the stream is important to quantify in order to understand better from where it came (e.g., Li et al. 2022; Naidu et al. 2022). Specifically, the chemical fingerprint of the OC stream, which has been relatively less explored than its kinematic signature, will offer a powerful tool in our hunt for the parent system (as it has for other systems, e.g., Aguado et al. 2021; Carrillo et al. 2022; Matsuno et al. 2022).

Therefore, in this work, we revisit the chemical properties of the OC stream with the newest data release (DR17) of the Sloan Digital Sky Survey's (SDSS; Gunn et al. 2006) Apache Point Observatory Galactic Evolution Experiment DR17 data (APOGEE; Nidever et al. 2015; Abdurro'uf et al. 2022; Blanton et al. 2017; Majewski et al. 2017; Wilson et al. 2019) survey in order to ascertain the possible parent population and provide chemical abundances for the largest sample of OC stars to date. To do this, we begin in Section 2, with a description of the exquisite data from the early third data release (EDR3) from the Gaia mission (Gaia Collaboration et al. 2021), which we use in order to select probable members of the OC stream (Section 2.1). We also describe the spectroscopic data from the APOGEE survey, where the stellar parameter and chemical abundance information for the OC stars are sourced (Section 2.2). In Section 3, we describe the chemical abundance patterns for stars in the OC stream and discuss these results in the context of probable parent populations in Section 4. We end by summarizing in Section 5.

2. Data

We use data from EDR3 of the European Space Agency's Gaia mission (Gaia Collaboration et al. 2021, 2016) crossmatched to DR17 of the APOGEE survey (Abdurro'uf et al. 2022; Majewski et al. 2017; Blanton et al. 2017), using the crossmatch provided by the APOGEE team and included in the DR17 data files. We use the astrometric data from Gaia to select members of the OC stream based on their kinematics, and use the element abundance measurements from the APOGEE survey to characterize the chemical properties of the stream.

2.1. Selection of Probable Orphan Stream Stars

Though candidate members of the OC stream were explicitly targeted in certain fields in the APOGEE-2 survey (ORPHAN-1 through ORPHAN-5; Zasowski et al. 2017), we search all APOGEE fields to identify candidate members with the hope of finding serendipitously targeted stream members. We start by selecting all APOGEE sources that match a set of expected stellar parameters for red giant branch (RGB) stars in the stellar halo. Based on the known distance trend of the stream from precise RR Lyrae (RRL) distance measurements (Koposov et al. 2019), we expect that only mid- to upper-RGB stars will be luminous enough to have been observed in the H band by APOGEE. So we first select only stars with surface gravities between $-0.5 < \log g < 2$ (with the lower limit primarily to remove missing values of -9999). We then transform the sky positions of the remaining APOGEE sources from equatorial coordinates to the OC stream coordinate frame defined in Koposov et al. (2019) and implemented in the `Gala` package (Price-Whelan 2017) to utilize the `astropy.coordinates` transformation framework (Astropy Collaboration et al. 2018).

To define criteria for selecting stream stars in sky position, proper motion components, and radial velocity, we use the candidate RRL and RGB star members of the OC stream from Koposov et al. (2019). In detail, as a function of OC stream longitude ϕ_1, we fit fifth-order polynomials to the sky position in OC stream latitude ϕ_2, the proper motion in stream longitude $\mu_{\phi_1^*}$ (including the $\cos\phi_2$ term), and the proper motion in stream latitude μ_{ϕ_2} using the OC RRL stars. Using these polynomial tracks, we select all APOGEE stars within $\pm 2.^\circ 5$ of the RRL track in ϕ_2, within ± 0.75 mas yr^{-1} of the RRL track in $\mu_{\phi_1^*}$, and within ± 0.5 mas yr^{-1} of the RRL track in μ_{ϕ_2}, where these widths were chosen to span the maximum dispersion of the RRL stars in each dimension. We then crossmatch the Koposov et al. (2019) RGB stream member stars to the SEGUE survey (Yanny et al. 2009) and fit a third-order polynomial to RGB stars with $v_{\rm helio} > 100$ kms^{-1} (to remove contamination; see the upper right panel of Figure 1) as

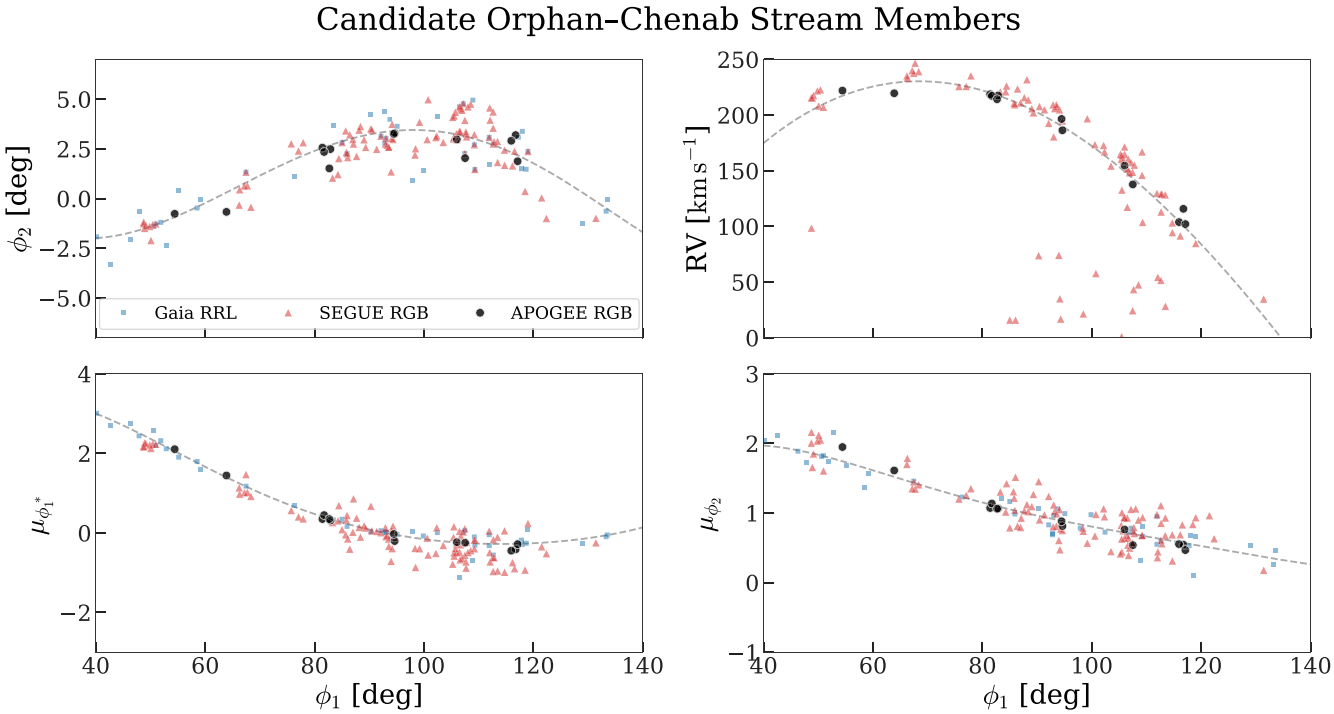

Figure 1. In all panels where values are available, the blue square markers show the OC stream RRL stars (Koposov et al. 2019) and the red triangles show the stream RGB stars (Koposov et al. 2019) crossmatched to the SEGUE survey. Sky positions (ϕ_1, ϕ_2) (in OC stream-aligned coordinates; Koposov et al. 2019) and proper motion components ($\mu_{\phi_1^*}$, μ_{ϕ_2}) are all taken from crossmatches with Gaia EDR3. Radial velocity (RV) measurements come from either APOGEE or SEGUE. The dashed lines show fifth- or third-order polynomial fits to the RRL (for the ϕ_2, $\mu_{\phi_1^*}$, and μ_{ϕ_2} panels) or RGB (for the RV panel) stars as a function of stream longitude ϕ_1. The black circle markers show the 13 stars identified as stream members from the APOGEE DR17 catalog as described in Section 2.1.

a function of ϕ_1. We finally select APOGEE stars with velocities within $\pm 20\,\mathrm{km\,s^{-1}}$ (about 5σ, using the velocity dispersion of the stream as measured in Li et al. 2022) of the RGB track in radial velocity.

Figure 1 summarizes our kinematic selection of OC stream members along with our final sample of APOGEE DR17 RGB stars. The styled markers in the figure show the three different data sets used here: the RRL and RGB candidate stream members from Koposov et al. (2019) are shown as blue (square) and red (triangle) markers, respectively, and the final sample of 13 APOGEE stars that are likely members of the OC stream are shown with the black (circle) markers.

2.2. Chemical Abundances from the APOGEE Survey

The APOGEE spectroscopic survey has collected more than 700,000 moderate-resolution ($R = \lambda/\Delta\lambda \sim 22{,}500$) near-infrared ($H$ band, 1.51–1.60 μm) spectra of mostly red giant stars across the Milky Way. The primary goal of the APOGEE survey is to study the kinematic and chemical properties of stars across the Milky Way to understand better its structure and nature. In recent years, the survey has also expanded to include red giant stars deep in the stellar halo and Galactic bulge in combination with the many stars it has already observed in the Galactic disk. The survey uses both the 2.5 m SDSS telescope at the Apache Point Observatory in the Northern Hemisphere and the 2.5 m du Pont telescope in the Southern Hemisphere.

The spectra obtained by the APOGEE survey have enabled the exploration of the detailed chemical properties of the Milky Way and its substructures. The APOGEE Stellar Parameter and Abundance Pipeline (ASPCAP; García Pérez et al. 2016) is the primary tool that has been used to derive both the atmospheric parameters ($T_{\rm eff}$, $\log g$, [Fe/H], microturblent velocity, and ξ) and chemical abundances for up to 20 elements (e.g., Holtzman et al. 2015, 2018; Abdurro'uf et al. 2022). These elements span the α (O, Mg, Ca, Si, Ti, and S), odd-Z (Al, K, and V), Fe-peak (Fe, Ni, Mn, Co, and Cr), and neutron-capture (Ce) groups. Currently, ASPCAP also allows for the derivation of heavier elements including s-process elements Nd, Ce, Rb, and Yb (e.g., Hawkins et al. 2016; Hasselquist et al. 2016; Cunha et al. 2017); however, only a relatively small fraction contains measurements of these elements from the current DR17 analysis (Blanton et al. 2017; Majewski et al. 2017; Holtzman et al. 2018; Abdurro'uf et al. 2022). While we provide a short description here, we refer the reader to García Pérez et al. (2016) and H. Jonsson et al. 2023, (in preparation), for a thorough description of ASPCAP. In order to measure the stellar properties, ASPCAP (as setup for APOGEE DR17 and for the data presented here) begins by first deriving the atmospheric parameters ($T_{\rm eff}$, $\log g$, and [Fe/H]) of the stars along with the [C/H], [N/H], and [α/Fe] values. This is done finding a best-matching spectrum (via χ^2 minimization) within an interpolated grid of synthetic spectra using the FERRE code (Allende Prieto et al. 2006; Zamora et al. 2015). The ξ parameter was determined through an empirically determine relationship with $\log g$.

Once this is complete, the ASPCAP pipeline derives stellar abundances by fitting models to the observed spectra in specific windows. Each window is weighted by its sensitivity to a given abundance and the how well the line modeled in Arcturus can be reproduced. Uncertainties in the stellar abundances are estimated using the scatter of each abundance within (assumed) chemically homogeneous open clusters. We refer the reader to

the APOGEE data release papers (Holtzman et al. 2015, 2018) for more details on the exact procedures.

In recent years, the OC stream was specifically targeted within the SDSS-IV APOGEE-2 survey. In order to obtain reliable stellar parameters and chemical abundances, we take the probable OC stream stars observed in APOGEE (described in Section 2.1) and apply several quality control cuts. Following other studies of distant systems (e.g., Hasselquist et al. 2021), we begin by selecting stars that have spectra with signal-to-noise ratios (S/Ns) of at least 70. We also remove stars that had the STAR_BAD bit set in the ASPCAPFLAG. These two criteria were employed to remove problematic or suspect stellar parameters and derived abundances, while attempting to keep the largest number of measurements. As noted in the APOGEE data release papers (e.g., Holtzman et al. 2015, 2018; García Pérez et al. 2016; Abdurro'uf et al. 2022), this is done in order ensure that the ASPCAP pipeline converged with no major warnings (e.g., if there were known issues with $T_{\rm eff}$, $\log g$, χ^2, rotation, S/N, if the derived parameters were near a grid edge, etc., the STAR_BAD flag would be set) indicating that the reported parameters and abundances may not be reliable. This cut reduced the sample from 13 probable OC members to 10. We also require that $3500 < T_{\rm eff} < 5500$ K and $\log g > 0.5$ dex, but all remaining OC member stars pass this selection. We note here that an additional four stars would be removed if we applied the more strict quality control cut that requires ASPCAPFLAG to equal 0 (i.e., absolutely no issues were raised in the ASPCAPFLAG pipeline). Even though the sample would be reduced, the results would remain unchanged.

In addition to the OC stream stars, for comparison, we also source the chemical abundance information of several globular clusters (specifically, we take members for the M107, M13, M71, M92, and M15 clusters from Mészáros et al. 2020) and dwarf galaxies (we take members of the Sagittarius dwarf galaxy from Hasselquist et al. 2021). These comparisons are on the same abundance scale as the OC stream stars and therefore give us a way to determine which chemical patterns are most similar.

3. Results: The Chemical Composition of OC Stream Stars

3.1. α elements (O, Mg, Ca, Si, S, and Ti)

The ratio of α elements with respect to iron, i.e., [O, Mg, Si, Ca, S, and Ti/Fe], are widely used in Galactic archeological studies because of their usefulness as a discriminator of the star formation history and past enrichment of the gas from which stars formed (e.g., Nomoto et al. 2013, and references therein). Additionally the [α/Fe] abundance ratio is thought to be sensitive to the ages of stars. This is because α elements are largely dispersed into the interstellar medium on short timescales by core-collapse Type II supernovae from massive stars. On the other hand, Fe and Fe-peak (Mn, Cr, Co, etc.) elements are dispersed by Type Ia supernovae, requiring a white dwarf. These occur on longer timescales (e.g., Gilmore & Wyse 1998; Matteucci & Recchi 2001; Maoz & Mannucci 2012) after Type II supernovae. Therefore, old stars will be enhanced in [α/Fe] but have low metallicities while younger stars (having been polluted by more Type Ia explosions) will be depleted in the [α/Fe] ratio but have higher metallicity. This creates a characteristic "knee" in the [α/Fe]–[Fe/H] plane. The metallicity at which this "knee" occurs is sensitive to the star formation rate (and thus mass) of the system in which the stars formed. For reference, the Milky Way has a "knee" in the [α/Fe]–[Fe/H] plane at [Fe/H] ~ -1.0 dex. This is in contrast to a much lower mass dwarf galaxy such as the Sculptor dwarf spheroidal galaxy, which has a lower [α/Fe] at a given metallicity compared to the Milky Way and potentially has a "knee" in the [α/Fe]–[Fe/H] plane at [Fe/H] ~ -1.87 dex (see Figure 3 of de Boer et al. 2014).

In Figure 2, we show the abundance ratios of O, Mg, Si, Ca, Ti, and S with respect to Fe as a function of [Fe/H], i.e., [O, Mg, Si, Ca, S, and Ti/Fe]. We note here that we specifically choose to plot the [Ti II/Fe] ratio within APOGEE rather than [Ti /Fe] due to known issues with the analysis of Ti I lines from the *H* band (e.g., see the discussions in Hawkins et al. 2016; Jönsson et al. 2018). In this figure (as well as Figure 4), the probable OC stream stars observed in the APOGEE survey (this study) are noted as black filled circles, while those observed in Casey et al. (2014) are shown as black open circles, and those from Ji et al. (2020) are shown as black open squares. As reference, we also show several comparison samples observed and analysed homogeneously within the APOGEE survey. These include a Milky Way sample[13] (shown as a blue-scaled background), several globular clusters (closed orange symbols), and candidate stars from the Sagittarius dwarf galaxy. The stellar clusters included are M107 (downward-pointing orange triangles), M13 (upward-pointing orange triangles), M71 (rightward-pointing orange triangles), M92 (leftward-pointing orange triangles), and M15 (orange diamonds).

It is clear from Figure 2 that the OC stream is not monometallic, as one might expect if it originates from a chemically homogeneous cluster of stars, and instead spans metallicities from $-2.10 <$ [Fe/H] < -1.50 dex. This result is similar to Casey et al. (2014) and Ji et al. (2020), who both study up to three stars each in the OC stream. In addition, we find that generally the ratio of α elements, specifically O, Mg, Si, Ca, Ti, and S, with respect to iron are lower in the OC stream stars compared to the homogeneously analysed Milky Way sample. However, we note here that there is significant scatter in the [Ca/Fe] abundance of OC stream stars in the APOGEE survey, which is not seen in the other data sets (Casey et al. 2014; Ji et al. 2020). This former point indicates that the stars in the OC stream were formed in an environment similar to a dwarf galaxy and not the Milky Way. In fact, taking the stars from this study and those of Casey et al. (2014) and Ji et al. (2020) together, one can conclude that the [α/Fe] abundance ratio[14] increases with decreasing metallicity with a plateau somewhere below [Fe/H]< -2.0 dex.

[13] As a simple Milky Way comparison sample, we select APOGEE stars with the same quality control cuts as in Section 2.2. We make an additional criteria to select Milky Way stars, namely that the absolute Galactic latitude, |b|, of the stars had to be less than 10°.

[14] There are various ways of defining (or measuring) the [α/Fe] abundance ratio. While APOGEE provides a globally derived [α/M] abundance ratio determined during the global spectral fitting procedure within the ASPCAP pipeline (i.e., the column labeled ALPHA_M in the APOGEE catalog), the literature studies (e.g., Casey et al. 2014), do not. Therefore, we compute, for each set of stars, a commonly derived [α/Fe] by averaging the [Mg/Fe], [Si/Fe], and [O/Fe] abundance ratios. The elements Mg, Si, and O were chosen because they are the best-measured α elements in APOGEE. We note that while the OC stars in APOGEE and Casey et al. (2014), have Mg, Si, and O measured, those in Ji et al. (2020) do not have Si measurements. As a result, we do not include the three stars from Ji et al. (2020) in the [α/Fe] (top panel), and HEx ratio (bottom panel) plots of Figure 3.

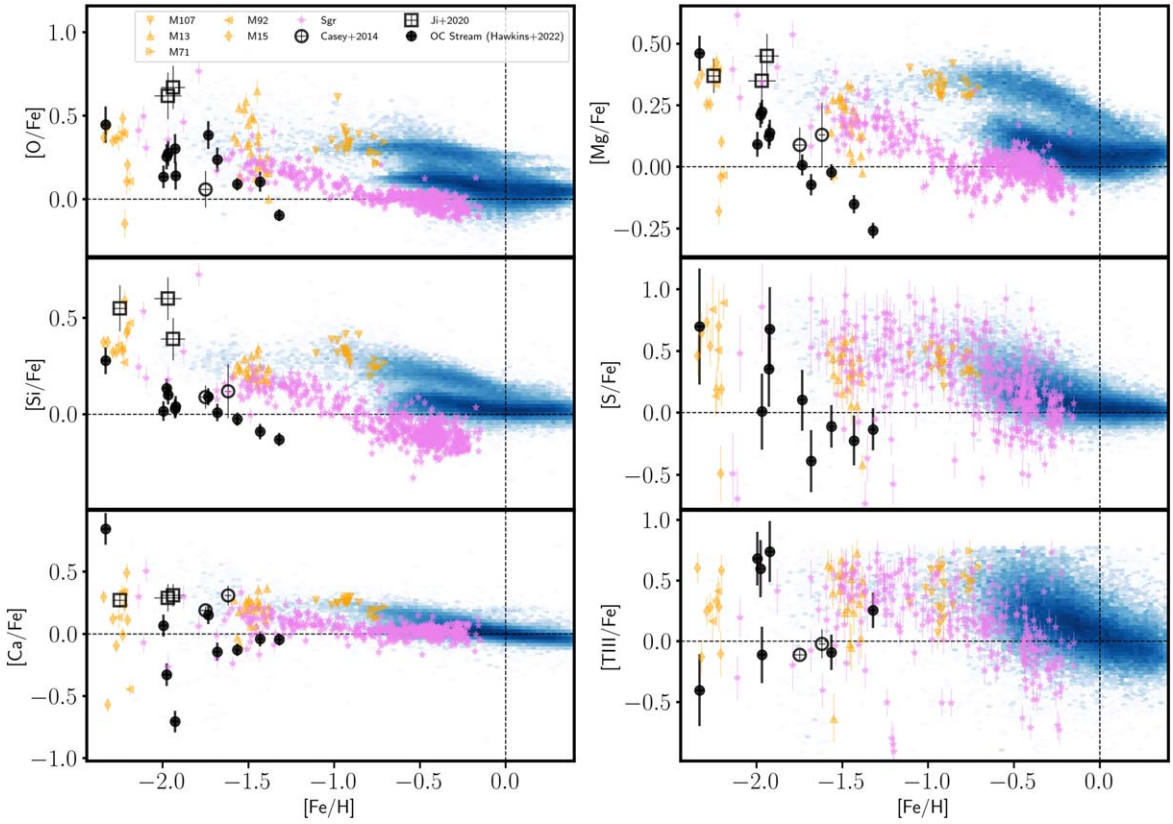

Figure 2. The α element abundance ratios (labeled on the vertical axis) as a function of iron abundance for OC stars observed in APOGEE (black circular markers), compared to the abundances of several stellar clusters that were derived consistently (orange markers), including M107 (upside-down triangles), M13 (triangles), M71 (rightward-pointing triangles), M82 (leftward-pointing triangles), and M15 (diamonds). In addition, we also show the abundances of a Milky Way comparison sample (with $|b| < 10°$, shown as the background density in blue) and Sagittarius dwarf (Hasselquist et al. 2021) galaxy stars (violet colored stars), all of which are observed and analysed homogeneously with the APOGEE survey. Finally the three highly probably OC stars studied in Casey et al. (2014) (open black circles) and Ji et al. (2020) (open black squares) are also shown.

We remind the reader that the location of the "knee" in the [α/Fe]–[Fe/H] plane, i.e., where the [α/Fe] begins to decrease with increasing metallicity rather than remaining flat, is directly related to the metal-enrichment achieved by a progenitor system at the time that Type Ia supernovae begin to contribute to the chemical evolution, and is therefore directly sensitive to the mass of the progenitor within which the stars were born (e.g., Tolstoy et al. 2009; de Boer et al. 2014, and references therein). The lack of a knee in the [α/Fe]–[Fe/H] plane (see the top panel of Figure 3) above [Fe/H] $\gtrapprox -2.0$ dex for OC stream stars, and the fact metallicity distribution is peaked at [Fe/H] $= -1.92$ dex with a dispersion of 0.28 dex, imply that the OC stream stars may originate in a system below the stellar mass of Sculptor ($M \lessapprox 1.7 \times 10^7\,M_\odot$) (e.g., Lianou & Cole 2013). This upper limit of $1.7 \times 10^7\,M_\odot$ for the progenitor of the OC stream is directly based on a relative comparison of the location of the "knee" in the [α/Fe]–[Fe/H] plane. This metallicity distribution is similar, but slightly metal-poorer, compared to earlier works (e.g., Li et al. 2022; Naidu et al. 2022). Additionally, the mean metallicity of the OC stream stars imply a progenitor mass of $\sim 8 \times 10^5\,M_\odot$ using the mass–metallicity relation of dwarf galaxies (Kirby et al. 2013). This lower limit mass for the progenitor of the OC stream assumes the $z = 0$ mass–metallicity relation for intact dwarf galaxies, which has found theoretically (e.g., Fattahi et al. 2020) and observationally (Kirby et al. 2013; Naidu et al. 2022). This value is not far, but slightly lower than the predicted upper limit of $\lessapprox 9.3 \times 10^6\,M_\odot$ from Grillmair et al. (2015) and the value of $4 \times 10^6\,M_\odot$ predicted from Koposov et al. (2019). More recently, Mendelsohn et al. (2022) estimated a total mass within 300 pc of $M = 1.1 \times 10^6\,M_\odot$, with a mass-to-light ratio of 74, for the OC stream progenitor. This mass value suggests a system much less massive than Sculptor, perhaps as low as the ultrafaint dwarf Leo IV (Strigari et al. 2008). However, we point out that while the current data imply this, we would recommend a more comprehensive study of the chemical properties of OC stream stars specifically in the metallicity range $-2.5 <$ [Fe/H] < -1.7 dex. Additional data in the regime would help pin down the exact location of any "knee" in the [α/Fe]–[Fe/H] diagram. We also note that while we assume here that the stream has the same progenitor metallicity, if the OC stars were stripped from a dwarf galaxy they may be more metal-poor than the actual parent system.

As is noted in Carlin et al. (2018), α elements can actually be separated into those formed during hydrostatic carbon and neon burning (Mg and O) and those formed in the explosion event of Type II supernovae (Si, Ca, and Ti). Those authors propose a useful abundance ratio constructed by taking the average abundances of the hydrostatic (Mg and O) α elements relative to their explosive counterparts (HEx ratio; Carlin et al. 2018). In the bottom panel of Figure 3, we further study the α elements by inspecting this HEx ratio ($[\alpha_{h/ex}]$) as a function of [Mg/H] (similar to Figure 4 of Carlin et al. 2018). We find that the Sgr stars in APOGEE from Hasselquist et al. (2021), which are a mix of stars in the main body and stream, show more scatter in [Mg/H] than the Sgr stream stars from

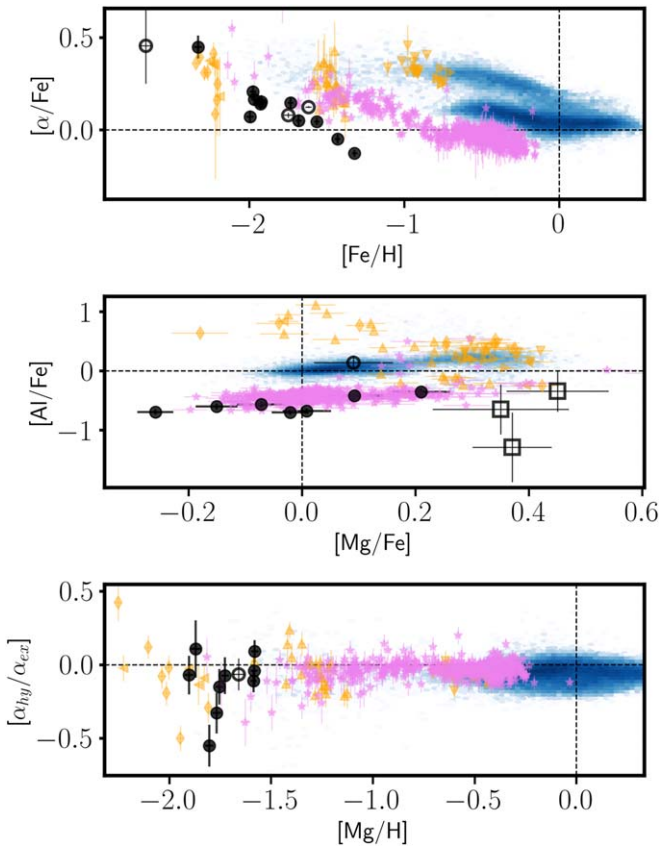

Figure 3. Top panel: the [α/Fe] abundance ratio as a function of [Fe/H]. Middle panel: [Al/Fe] as a function of [Mg/Fe], showing that the OC stream stars do not behave as one would expect from globular cluster stars. Bottom panel: the so-called Hex abundance ratio as a function of [Fe/H]. The Hex ratio and its importance is described in the text and in Carlin et al. (2018). In all panels, the symbols are the same as in Figure 2.

Carlin et al. (2018), but similarly show a collective trend of HEx ratios less than zero; this trend supports a scenario in which Sgr initially had very few massive stars. The HEx ratio for the OC stream stars also decreases with [Mg/H] and shows a downturn at a roughly constant value of [Mg/H] ~ -2, which would correspond to a decrease in stars formed during hydrostatic burning at that (very low) level of Mg enrichment.

3.2. Odd-Z Elements (Al, K,and V)

The *H*-band spectra observed within the APOGEE survey allow for the measurement of several odd-*Z* elements including Al, K, and V. We note that there are Na lines found in the *H*-band spectra, however they were not well measured for each of the OC stream stars, so we choose to not report or discuss them here. While the various odd-*Z* elements have different production sites, they still provide useful diagnostics of the environment from where the OC stream originated.

For example, Al, often known as a "mild α element", is thought to be produced (similarly to hydrostatic α elements) during carbon and neon burning in massive stars; however, it is also produced in the Mg–Al cycle in AGB stars (e.g., Samland 1998; Doherty et al. 2014; Smiljanic et al. 2016). Upon production, Al is dispersed into the interstellar medium through both Type II supernovae and through the winds of AGB stars. Interestingly, Al seems to be a key element for distinguishing stars originating in the second generation of stars formed in globular clusters through the Mg–Al anticorrelation (e.g., Carretta et al. 2009b, 2009a; Mészáros et al. 2015; Pancino et al. 2017). This particular feature, though not necessarily present in all globular clusters, manifests as a group of stars with significant enhancements of Al (often reaching values as high as [Al/Fe] ~ 1.0 dex) and which simultaneously have a depletion in [Mg/Fe]. The results for the [Mg/Fe] and [Al/Fe] abundance results can be found in Figures 2 and 4, respectively. However it is more useful to view the [Mg/Fe] as a function of [Al/Fe] for the purpose of looking for potential globular clusters (e.g., see Figure 3 of Pancino et al. 2017). This can be found in the middle panel of Figure 3. It clearly shows that the OC stars are not enhanced in [Al/Fe] and are, in fact, significantly depleted. Additionally [Al/Fe] is lower than expected for the various globular clusters observed in the APOGEE survey.

K is probably produced in explosive oxygen burning in Type II supernovae. It is observationally expected to increase with decreasing metallicity, similar to α elements, also dispersed in similar explosions (Hawkins et al. 2016). The [K/Fe] abundances of the OC stream stars (Figure 4) observed in APOGEE seem to have significant scatter. This large scatter is not seen in the sample observed in Casey et al. (2014) with optical spectra.

The production site for V is poorly modeled in supernovae yields. Currently, it is thought that V is produced in explosive oxygen, silicon, and neon burning in both Type II and Type Ia supernovae (e.g., Samland 1998). Theoretically, [V/Fe] is expected to increase with decreasing metallicity. This is seen within the Milky Way sample as well as the OC stream stars. However, we find in Figure 4 that the OC stream stars have lower [V/Fe] compared to the Milky Way or known clusters at a given metallicity .

3.3. Iron-peak Elements (Mn, Co, Cr, and Ni)

The Fe-peak elements observed within the APOGEE survey include Mn, Co, Cr, and Ni. While these elements are thought to be produced and dispersed largely through Type Ia explosions, many of these Fe-peak elements are also produced in Type II supernova expositions (Iwamoto et al. 1999; Kobayashi et al. 2006; Kobayashi & Nomoto 2009; Nomoto et al. 2013, and references therein). The [Mn, Co, Cr, and Ni/Fe] abundance ratios of the Fe-peak elements as a function of metallicity for the OC stream (and comparison sample) stars can be found in Figure 4.

Mn is thought to be produced in significantly higher amounts in Type Ia supernovae compared to Fe and is therefore a good tracer of such explosions. However, unlike many of the other Fe-peak elements, it is expected (and observed) that the abundance ratio [Mn/Fe] decreases with decreasing metallicity in the Milky Way. This pattern could be due to a metallically dependence on the yields of Mn or a delay in enrichment from Type Ia supernovae (e.g., Kobayashi et al. 2006; Feltzing et al. 2007). As expected, in the Milky Way (blue scale hexagonal bins in Figure 4) [Mn/Fe] does decrease with decreasing metallicity. We find a relatively constant subsolar [Mn/Fe] for most OC stream stars although with significant scatter. This is in contrast to the results of Casey et al. (2014) and Ji et al. (2020), who both show a decreasing trend in [Mn/Fe] with metallicity, albeit offset from each other and with small samples (there are only two OC stream stars both optical studies which have measured Mn abundances). Further, we find

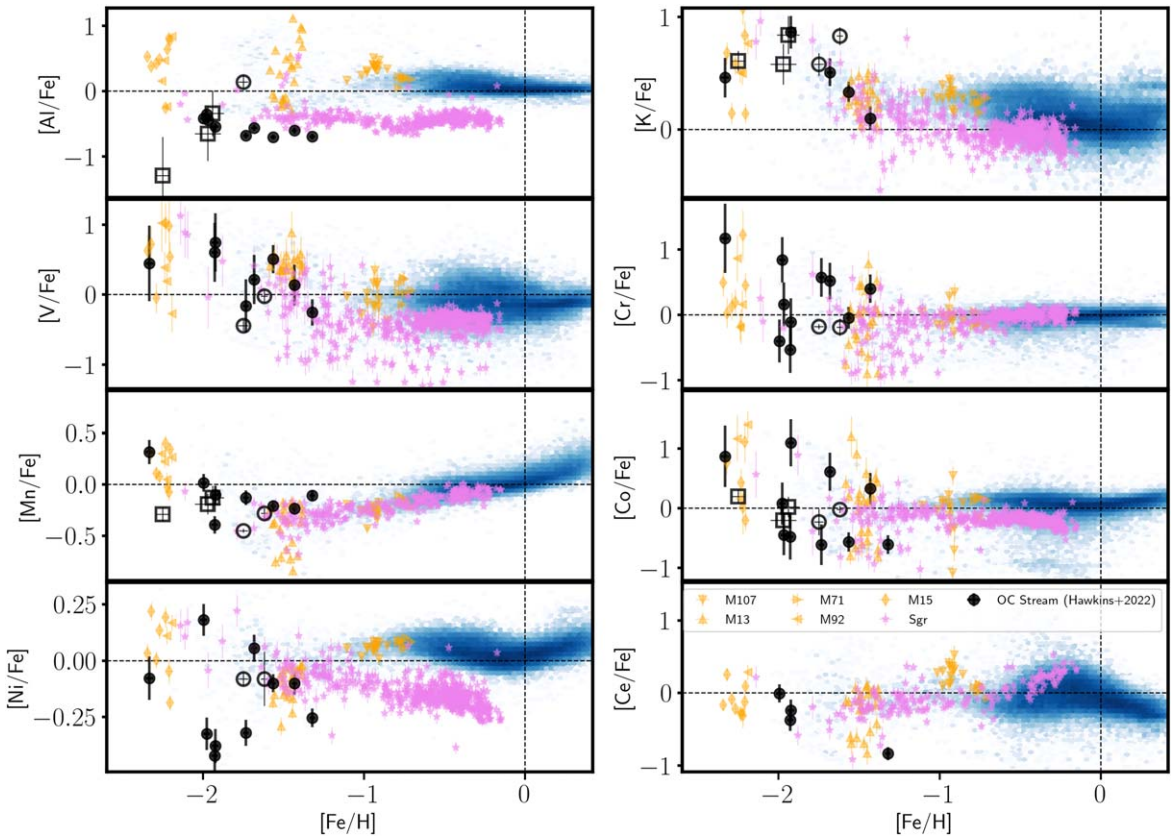

Figure 4. Left panel: the same as Figure 2, but for [Al/Fe], [V/Fe], [Mn/Fe], and [Ni/Fe] from top to bottom, respectively. Right panel: the same as Figure 2, but for [K/Fe], [Cr/Fe], [Co/Fe], and [Ce/Fe] from top to bottom, respectively.

that [Mn/Fe] is slightly higher in the OC stream compared to both the Milky Way and Sgr at similar metallicities.

Cr and Ni are thought to be produced in similar ways (and levels) as Fe in Type Ia supernovae. Therefore it is both expected and observed that Cr and Ni track Fe in lockstep (i.e., the [Ni/Fe] and [Cr/Fe] values are fairly constant over a broad range in [Fe/H]). This is observed for both the OC stream stars and the comparison samples, albeit with moderate dispersion. We also find that [Ni/Fe] for the OC stars is slight lower compared to Milky Way and Sgr stars. Recent studies of Mn and Ni abundance patterns in dwarf galaxies (e.g., Sanders et al. 2021), have shown that sub-Chandrasekhar mass systems are a significant contributor to Type Ia supernova in metal-poor, dwarf-galaxy-like environments. We find abundance patterns (e.g., subsolar [Ni/Fe] and [Mn/Fe]) that are consistent with this.

Finally, the production of Co, while similar to Cr and Ni, is through both Type Ia and Type II supernovae. However unlike Cr and Ni, the amount of Co produced in these explosions is thought to depend on both mass and metallicity (Kobayashi et al. 2006) and therefore the [Co/Fe] ratio increases with decreasing metallicity for subsolar [Fe/H]. This abundance pattern is seen in the comparison samples as well the OC stream stars, which is not seen in the stars where Co could be measured in Casey et al. (2014). We also note in all of the Fe-peak elements the OC stream stars could not really be distinguished from the comparison Milky Way sample in mean or dispersion.

3.4. S-process Elements (Ce)

It was noted in Hawkins et al. (2016) that the *H*-band spectra obtain by APOGEE contain *s*-process information in addition to the α element, Fe-peak, and odd-*Z* elements that had been known before (e.g., Holtzman et al. 2015). They identified Rb, Nd, and Yb but noted that each were difficult to measure at the resolution. Following this, Hasselquist et al. (2016, 2021) identified and measured Nd in the core of the Sagittarius dwarf galaxy and Cunha et al. (2017) identified several Ce lines within the APOGEE spectra. We checked whether Ce and Nd were measured in any of the OC stream stars with the ASPCAP pipeline. We found in each case that Nd could not be measured in such low-metallicity stars given the very weak line strength. Ce, on the other hand, could be measured for four stars. In the bottom right panel of Figure 4, we show the [Ce/Fe] abundance ratio as a function of [Fe/H] for OC stream stars (red circles), compared to other Milky Way stars (blue-scaled background), globular clusters (orange symbols), and Sagittarius dwarf galaxy (magenta stars) stars. The [Ce/Fe] for values are on the lower end (all showing negative [Ce/Fe] values) compared to those found in halo field stars of similar metallicity (e.g., see Figure 7 of Cunha et al. 2017). We note however that spectra with higher S/Ns for many more OC stream stars will be required to draw any conclusions.

4. Discussion

In this section, we contextualize the chemical abundance patterns for OC stream stars and what it can tell us about what

the parent population may (or may not) be. Namely, in Section 4.1 we evaluate the hypothesis that the OC stream was created by a fully disrupted globular cluster. In Section 4.2, we contrast that scenario with the idea that the OC stream was created by a disrupted dwarf galaxy.

4.1. Ruling Out a Globular Cluster Origin

Globular clusters are old, metal-poor relics that contain many (10^4–10^6) stars. It has been shown that several globular clusters in the Milky Way halo are being tidally disrupted by the Milky Way (e.g., the tidal tails around Palomar 5 and Palomar 13; Odenkirchen et al. 2003; Shipp et al. 2020). It is therefore possible that the OC stream could be produced by a relic globular cluster. Koposov et al. (2019) notes that seven globular clusters are within 7° of the stream's great circle.

There are a handful of globular clusters that have been mentioned in the literature that could be associated with the OC stream. These include several clusters that have already been discussed in the literature as possible parents for the OC stream, namely NGC 2419 (discussed in Brüns & Kroupa 2011), Ruprecht 106 (discussed in Grillmair et al. 2015), and Laevens 3 (Li et al. 2022). In the first two cases the authors conclude that while these clusters are close to the stream (Ruprecht 106 being the closest; Grillmair et al. 2015; Koposov et al. 2019), they are not likely to be associated with it, which we confirm here.

From the perspective of chemical abundance patterns, we are in a position to evaluate the claim that the OC stream could originate from a globular cluster. First, from Section 3, we show that the OC stream is not monometallic and has considerable scatter in many abundances. This rules out a chemically homogeneous globular cluster formation scenario. Given that Ruprecht 106 has been shown likely to be a single population, chemically homogeneous globular cluster (Villanova et al. 2013), we rule out this cluster as a potential parent.

However, we know that not all globular clusters are monometallic and those which are not have second-generation stars which often display anticorrelations between Mg–Al and Na–O (e.g., Carretta et al. 2009b, 2009a; Mészáros et al. 2015; Pancino et al. 2017; Bastian & Lardo 2018). In these clusters it is expected that [Al/Fe] is enhanced while [Mg/Fe] is depleted in the second-generation stars. In Figure 3, we clearly show that none of the OC stream stars display such chemical signatures.

Furthermore, NGC 2419, a cluster said to be a potential parent to the OC stream (Brüns & Kroupa 2011), has been shown to have a unique anticorrelation between [K/Fe] and [Mg/Fe] (Cohen et al. 2011; Mucciarelli et al. 2012). These authors found that NGC 2419 has stars which have simultaneously high K (with [K/Fe] > 1) and low Mg (with [Mg/Fe] < 0). Similar to Casey et al. (2014), we find that [K/Fe] is too low to be consistent with this globular cluster. We therefore rule out this cluster as a potential parent.

Finally, Laevens 3 was proposed by Li et al. (2022) as a potential parent progenitor of the OC stream. Only one detailed chemical study of the Laevens 3 cluster exists (Longeard et al. 2019), which explored the metallicity and [α/Fe] for a total of three member stars. The metallicity they derive for the cluster is [Fe/H] $= -1.8 \pm 0.10$ dex and a metallicity dispersion of σ[Fe/H] < 0.50 dex. Additionally, they find [α/Fe] $= 0.00 \pm 0.20$ dex. The APOGEE OC stream stars have a median metallicity of -1.92 with a dispersion of $\sim$0.28 dex. While the metallicity is consistent with those of Laevens 3 the mean [α/Fe] of Laevens 3 is 0.00 dex, while the OC stream stars have a significantly higher mean [α/Fe] of 0.15 dex. Given this, we note that Laevens 3 is not a likely parent of the OC stream. However we note that a more detailed chemical characterization of Laevens 3 and the OC stream would be helpful to illustrate this further.

Given that none of the globular clusters that are close to the OC stream match its phase-space tracks (Koposov et al. 2019), as well as the chemical abundance information presented here and in Casey et al. (2014), the lack of an Mg–Al or K–Mg anticorrelation, and the spread in [Fe/H], we determine that it is unlikely that the parent of the OC stream is a globular cluster.

4.2. Dwarf Galaxy Origins for the OC Stream

In the last section, consistent with results on a smaller sample of stars from Sesar et al. (2013) and Casey et al. (2014), we conclude that the OC stream could not have originated from a disrupting globular cluster. Therefore, in this section, we evaluate the possibility that the OC stream has originated from a dwarf galaxy system (including ultrafaint and classical dwarfs). The upper (defined by the "knee" in the [α/Fe]–[Fe/H] plane) and lower (defined by the mass–metallicity relation) limits on the mass of the progenitor are $8 \times 10^5 \lessapprox M \lessapprox 1 \times 10^7\, M_\odot$. The lower end of this limit is consistent with the inferred stellar mass ($\sim 10^6\ M_\odot$) of the progenitor of the OC stream from recent studies (e.g., Mendelsohn et al. 2022; Naidu et al. 2022). While it is possible that the progenitor of the OC stream has been fully (or mostly) dissolved, given that the stream stellar mass is of order $5.6 \times 10^6\, M_\odot$ (Koposov et al. 2023), it is not likely that its massive progenitor still exists. Given that several currently surviving dwarfs galaxies have been identified as potential progenitors, we discuss them below.

In Koposov et al. (2019), it is noted that there are three ultrafaint dwarf galaxies (Segue 1, Ursa Major II, and Grus II) and one classical dwarf spheroidal galaxy (Leo I) in the vicinity of the OC stream. Of these, Leo I is automatically ruled out because it is much farther away ($\sim$250 kpc) compared to the stream and thus they are not likely physically associated (Koposov et al. 2019). We do not discuss Leo I further for this reason.

In recent works (e.g., Casey et al. 2014), it was discussed that the OC stream progenitor could be the Segue 1 dwarf spheroidal. With the chemical characterization in this work, we are in a position to assess this as a possibility. The chemical patterns of the Segue 1 dwarf spheroidal were studied in Frebel et al. (2014). In that work, they indicated that Segue 1 is one of the only dwarf galaxy systems where the ratios of [Mg, Si, and Ca/Fe] are actually enhanced and show no evidence for a "knee". This is inconsistent with the abundance patterns seen in Section 3.1, where we find that the [Mg, Si, and Ca/Fe] abundance ratios are not only depleted relative to the rest of the Milky Way halo but they also increase with decreasing metallicity, indicating there is likely a "knee" below [Fe/H] < -2 dex. Assuming that the chemical pattern observed in the OC stream should be drawn from the chemical makeup of its progenitor, our results rule out Segue 1 a possible progenitor to the OC stream.

Ursa Major II has also been discussed as a potential parent of the OC stream (Fellhauer et al. 2007). Kirby et al. (2008) was among the first to derive chemical abundance information, though only [Fe/H]. They found in that work that Ursa Major II has a mean metallicity of [Fe/H] ~ -2.44 dex with a spread of 0.57 dex. The first detailed chemical

abundance study of Ursa Major II was done by Frebel et al. (2010); however, in that work they only obtained chemical abundances for three stars and each of those stars happened to have metallicities of $[Fe/H] < -2.3$ dex (significantly lower than the [Fe/H] of the OC stream stars discussed in this work).

Another dwarf galaxy has been recently presented (e.g., Erkal et al. 2019; Koposov et al. 2019) as a potential parent of the OC stream, namely the Grus II system. The Grus II system is an ultrafaint dwarf galaxy at distance of ∼49 kpc from the Galactic center and an estimated physical size of ∼93 pc (Drlica-Wagner et al. 2015). To date, the chemical pattern of Grus II is still poorly constrained. Hansen et al. (2020) completed the first and only detailed chemical study of three of the brightest members of Grus II, which were in the metallicity range $-2.95 < [Fe/H] < -2.49$ dex. If this metallicity range is representative of Grus II, it would indicate that the either Grus II has a very large metallicity spread or that the OC stream is likely too metal-rich to have originated within Grus II. Further chemical characterization of Grus II as a more metal-rich (i.e., $[Fe/H] > -2.10$ dex) dwarf galaxy would be a necessary step to determine if it is connected to the OC stream. With limited chemical abundance information from Grus II, Ursa Major II, and the OC stream, we recommend detailed chemical abundance studies in overlapping metallicity regimes for each in order to distinguish which could be the parent. We note here that all of the dwarf galaxies listed here are likely offset from the OC stream in at least one component of its track (e.g., Koposov et al. 2019) or the chemical pattern does not match, which illustrates that the hunt for a progenitor is still ongoing. Further chemo-dynamic tagging using both the chemical fingerprint and the dynamical properties (in integral of motion space) of the OC stream and of nearby dwarf galaxies, such as Grus II, will be essential in future studies. The chemical patterns presented in this work will help identify a progenitor.

5. Summary

The OC stream is an relatively old, fairly narrow stream of stars found around the Milky Way (e.g., Grillmair 2006; Belokurov et al. 2007) with no known progenitor system. Recently, the kinematics of the OC stream has been studied and modeled using data from the second data release of the all-sky Gaia survey (Erkal et al. 2019; Fardal et al. 2019; Koposov et al. 2019). These studies have furthered our knowledge of the spatial and dynamical properties of this interesting object. An interesting but still rather unexplored avenue to help find the parent of the OC stream lies in matching its detailed chemical abundance pattern to possible progenitor systems.

Only two studies currently exist regarding the detail abundances of at most six probable OC stream members (Casey et al. 2014; Ji et al. 2020). In this work, we use the updated kinematic and spatial properties of the OC stream to find 13 probable OC stream stars within the APOGEE survey. The APOGEE survey contains moderate-resolution, *H*-band spectra for more than a few times 10^5 stars. These spectra enable the atmospheric ($T_{\rm eff}$ and $\log g$) and chemical characterization of the stars in various elemental families including the α element (O, Mg, Ca, Si, Ti, and S), odd-*Z* (Al, K, V), and Fe-peak (Fe, Ni, Mn, Co, and Cr) families. Of the 14 probable OC stream stars, five have measured stellar parameters and chemical abundances in the APOGEE survey. This represents the largest study of the chemical abundance pattern of the OC stream and the first with a large spectroscopic survey in the infrared.

Our results can be summarized as follows:

1. The metallicity of the OC stream ranges at least from $-2.10 < [Fe/H] < -1.55$ dex, indicating that is not monometallic, consistent with other findings (Casey et al. 2014). We also find that in many of the elements studied, that the OC stream is not a monoabundance population.
2. The α elements are largely depleted compared to the Milky Way reference sample at similar metallicities (Figure 2 and top panel of Figure 3). This result is particularly important because it indicates that the stars that make up the OC stream have not likely originated in the Milky Way. Instead, they have come from an environment with a lower star formation rate (e.g., dwarf spheroidal or ultrafaint dwarf galaxies).
3. The distribution of OC stars in the [α/Fe]–[Fe/H] abundance plane seems to indicate that the OC stream has no reasonable "knee" at [Fe/H] larger than −2.0 dex, implying an upper limit on the mass of its progenitor of $M \lessapprox 1.4 \times 10^7\,M_\odot$. We emphasize, however, that many more stars with $[Fe/H] < -2$ dex are needed to pin down if and at what metallicity a "knee" can be found. The metallicity distribution combined with the [α/Fe] abundances suggest the OC progenitor should be between $8 \times 10^5 \lessapprox M \lessapprox 1 \times 10^7\,M_\odot$.
4. Studying the abundance patterns of Mg and Al (in Figure 3) indicates that stars making up the OC stream stars are not consistent with originating in a known globular cluster, consistent with other findings (e.g., Casey et al. 2014; Ji et al. 2020).
5. We find that the dispersions in many Fe-peak elements (Mn, Cr, and Ni) are significantly larger than what is found with three OC stream candidate stars from Casey et al. (2014) and those of Ji et al. (2020). This discrepancy underscores the need for significantly larger samples of stars within the OC stream in order to constrain the nature of its chemical pattern elements further. Interestingly, we also find that the OC stream is offset in some Fe-peak elements (e.g., Ni and Mn) compared to the Milky Way.

We are currently working on two paths forward based on these results. First, we need to evaluate further the claim that the Grus II dwarf spheroidal could be a potential parent for the OC stream. In order to test this properly, we are working to obtain high-resolution spectra of tens of stars within Grus II to determine if its metallicity and chemical abundance patterns are consistent with the OC stream. An initial chemical study of three stars in Grus II was carried out by Hansen et al. (2020). These authors found that Grus II is very metal-poor (i.e., $-2.49 < [Fe/H] < -2.94$ dex) and has a chemical pattern (elevated [Mg/Ca] ratios) that suggest it likely had a top-heavy initial mass function. It is clear that a larger study of the system focusing on candidates at higher metallicities (ones that overlap with the OC) stream is required. Further, kinematic and dynamical studies of all potential progenitors that include the impact of the Large Magellanic Cloud (e.g., Lilleengen et al. 2023, S. Koposov et al., in preparation), should be done in order to confirm any potential progenitor of the OC stream. While in this work, we have further advanced our

understanding of the chemical nature of the OC stream by increasing the sample size by a factor of two, we still have only relatively small numbers. Therefore, we also recommend exploring the chemical pattern of 24 OC stream candidate found in the LAMOST survey (e.g., Li et al. 2017) using advanced spectral analysis techniques such as The Payne (Ting et al. 2017).

K.H. acknowledges support from the National Science Foundation grants AST-1907417 and AST-2108736 and from the Wootton Center for Astrophysical Plasma Properties funded under the United States Department of Energy collaborative agreement DE-NA0003843. This work was performed in part at Aspen Center for Physics, which is supported by the National Science Foundation grant PHY-1607611. This work was performed in part at the Simons Foundation Flatiron Institute's Center for Computational Astrophysics during K.H.'s tenure as an IDEA Fellow. C.L. acknowledges funding from the European Research Council (ERC) under the European Unions Horizon 2020 research and innovation program (grant agreement No. 852839).

A.A.S. and A.Z.S. acknowledge support from the SDSS FAST Initiative (https://www.sdss.org/education/faculty-and-student-team-fast-initiative/), in particular funding for the CUNY FAST group.

This work has made use of data from the European Space Agency (ESA) mission Gaia (https://www.cosmos.esa.int/gaia), processed by the Gaia Data Processing and Analysis Consortium (DPAC, https://www.cosmos.esa.int/web/gaia/dpac/consortium). Funding for the DPAC has been provided by national institutions, in particular the institutions participating in the Gaia Multilateral Agreement.

Funding for the Sloan Digital Sky Survey IV has been provided by the Alfred P. Sloan Foundation, the U.S. Department of Energy Office of Science, and the Participating Institutions.

SDSS-IV acknowledges support and resources from the Center for High Performance Computing at the University of Utah. The SDSS website is www.sdss.org.

SDSS-IV is managed by the Astrophysical Research Consortium for the Participating Institutions of the SDSS Collaboration including the Brazilian Participation Group, the Carnegie Institution for Science, Carnegie Mellon University, Center for Astrophysics | Harvard & Smithsonian, the Chilean Participation Group, the French Participation Group, Instituto de Astrofísica de Canarias, The Johns Hopkins University, Kavli Institute for the Physics and Mathematics of the Universe (IPMU) / University of Tokyo, the Korean Participation Group, Lawrence Berkeley National Laboratory, Leibniz Institut für Astrophysik Potsdam (AIP), Max-Planck-Institut für Astronomie (MPIA Heidelberg), Max-Planck-Institut für Astrophysik (MPA Garching), Max-Planck-Institut für Extraterrestrische Physik (MPE), National Astronomical Observatories of China, New Mexico State University, New York University, University of Notre Dame, Observatário Nacional / MCTI, The Ohio State University, Pennsylvania State University, Shanghai Astronomical Observatory, United Kingdom Participation Group, Universidad Nacional Autónoma de México, University of Arizona, University of Colorado Boulder, University of Oxford, University of Portsmouth, University of Utah, University of Virginia, University of Washington, University of Wisconsin, Vanderbilt University, and Yale University.

ORCID iDs

Keith Hawkins https://orcid.org/0000-0002-1423-2174
Adrian M. Price-Whelan https://orcid.org/0000-0003-0872-7098
Allyson A. Sheffield https://orcid.org/0000-0003-2178-8792
Aidan Z. Subrahimovic https://orcid.org/0000-0002-0837-6331
Rachael L. Beaton https://orcid.org/0000-0002-1691-8217
Vasily Belokurov https://orcid.org/0000-0002-0038-9584
Denis Erkal https://orcid.org/0000-0002-8448-5505
Sergey E. Koposov https://orcid.org/0000-0003-2644-135X
Richard R. Lane https://orcid.org/0000-0003-1805-0316
Christian Nitschelm https://orcid.org/0000-0003-4752-4365

References

Abdurro'uf, Accetta, K., Aerts, C., et al. 2022, ApJS, 259, 35
Aguado, D. S., Myeong, G. C., Belokurov, V., et al. 2021, MNRAS, 500, 889
Allende Prieto, C., Beers, T. C., Wilhelm, R., et al. 2006, ApJ, 636, 804
Astropy Collaboration, Price-Whelan, A. M., Sipőcz, B. M., et al. 2018, AJ, 156, 123
Banik, N., Bovy, J., Bertone, G., Erkal, D., & de Boer, T. J. L. 2021, MNRAS, 502, 2364
Bastian, N., & Lardo, C. 2018, ARA&A, 56, 83
Belokurov, V., Evans, N. W., Irwin, M. J., et al. 2007, ApJ, 658, 337
Belokurov, V., Zucker, D. B., Evans, N. W., et al. 2006, ApJL, 642, L137
Blanton, M. R., Bershady, M. A., Abolfathi, B., et al. 2017, AJ, 154, 28
Bonaca, A., Conroy, C., Wetzel, A., Hopkins, P. F., & Kereš, D. 2017, ApJ, 845, 101
Bonaca, A., Geha, M., & Kallivayalil, N. 2012, ApJL, 760, L6
Bonaca, A., Hogg, D. W., Price-Whelan, A. M., & Conroy, C. 2019, ApJ, 880, 38
Bonaca, A., Pearson, S., Price-Whelan, A. M., et al. 2020, ApJ, 889, 70
Brüns, R. C., & Kroupa, P. 2011, ApJ, 729, 69
Bullock, J. S., & Johnston, K. V. 2005, ApJ, 635, 931
Carlberg, R. G., Grillmair, C. J., & Hetherington, N. 2012, ApJ, 760, 75
Carlin, J. L., Sheffield, A. A., Cunha, K., & Smith, V. V. 2018, ApJL, 859, L10
Carretta, E., Bragaglia, A., Gratton, R., & Lucatello, S. 2009a, A&A, 505, 139
Carretta, E., Bragaglia, A., Gratton, R. G., et al. 2009b, A&A, 505, 117
Carrillo, A., Hawkins, K., Jofré, P., et al. 2022, MNRAS, 513, 1557
Casey, A. R., Keller, S. C., Da Costa, G., Frebel, A., & Maunder, E. 2014, ApJ, 784, 19
Cohen, J. G., Huang, W., & Kirby, E. N. 2011, ApJ, 740, 60
Cooper, A. P., Parry, O. H., Lowing, B., Cole, S., & Frenk, C. 2015, MNRAS, 454, 3185
Cunha, K., Smith, V. V., Hasselquist, S., et al. 2017, ApJ, 844, 145
Davis, M., Efstathiou, G., Frenk, C. S., & White, S. D. M. 1985, ApJ, 292, 371
de Boer, T. J. L., Belokurov, V., Beers, T. C., & Lee, Y. S. 2014, MNRAS, 443, 658
Doherty, C. L., Gil-Pons, P., Lau, H. H. B., Lattanzio, J. C., & Siess, L. 2014, MNRAS, 437, 195
Drlica-Wagner, A., Bechtol, K., Rykoff, E. S., et al. 2015, ApJ, 813, 109
Erkal, D., Belokurov, V., Bovy, J., & Sanders, J. L. 2016, MNRAS, 463, 102
Erkal, D., Belokurov, V., Laporte, C. F. P., et al. 2019, MNRAS, 487, 2685
Erkal, D., Koposov, S. E., & Belokurov, V. 2017, MNRAS, 470, 60
Fardal, M. A., van der Marel, R. P., Sohn, S. T., & del Pino Molina, A. 2019, MNRAS, 486, 936
Fattahi, A., Deason, A. J., Frenk, C. S., et al. 2020, MNRAS, 497, 4459
Fellhauer, M., Evans, N. W., Belokurov, V., et al. 2007, MNRAS, 375, 1171
Feltzing, S., Fohlman, M., & Bensby, T. 2007, A&A, 467, 665
Frebel, A., Simon, J. D., Geha, M., & Willman, B. 2010, ApJ, 708, 560
Frebel, A., Simon, J. D., & Kirby, E. N. 2014, ApJ, 786, 74
Gaia Collaboration, Brown, A. G. A., Vallenari, A., et al. 2016, A&A, 595, A2
Gaia Collaboration, Brown, A. G. A., Vallenari, A., et al. 2021, A&A, 649, A1

García Pérez, A. E., Allende Prieto, C., Holtzman, J. A., et al. 2016, AJ, 151, 144
Gibbons, S. L. J., Belokurov, V., & Evans, N. W. 2014, MNRAS, 445, 3788
Gilmore, G., & Wyse, R. F. G. 1998, AJ, 116, 748
Gilmore, G., Koposov, S., Norris, J. E., et al. 2013, Msngr, 151, 25
Grillmair, C. J. 2006, ApJL, 645, L37
Grillmair, C. J., Hetherington, L., Carlberg, R. G., & Willman, B. 2015, ApJL, 812, L26
Gunn, J. E., Siegmund, W. A., Mannery, E. J., et al. 2006, AJ, 131, 2332
Hansen, T. T., Marshall, J. L., Simon, J. D., et al. 2020, ApJ, 897, 183
Hasselquist, S., Hayes, C. R., Lian, J., et al. 2021, ApJ, 923, 172
Hasselquist, S., Shetrone, M., Cunha, K., et al. 2016, ApJ, 833, 81
Hawkins, K., Kordopatis, G., Gilmore, G., et al. 2015, MNRAS, 447, 2046
Hawkins, K., Masseron, T., Jofré, P., et al. 2016, A&A, 594, A43
Helmi, A., & de Zeeuw, P. T. 2000, MNRAS, 319, 657
Holtzman, J. A., Hasselquist, S., Shetrone, M., et al. 2018, AJ, 156, 125
Holtzman, J. A., Shetrone, M., Johnson, J. A., et al. 2015, AJ, 150, 148
Iwamoto, K., Brachwitz, F., Nomoto, K., et al. 1999, ApJS, 125, 439
Ji, A. P., Li, T. S., Hansen, T. T., et al. 2020, AJ, 160, 181
Jönsson, H., Allende Prieto, C., Holtzman, J. A., et al. 2018, AJ, 156, 126
Kirby, E. N., Cohen, J. G., Guhathakurta, P., et al. 2013, ApJ, 779, 102
Kirby, E. N., Simon, J. D., Geha, M., Guhathakurta, P., & Frebel, A. 2008, ApJL, 685, L43
Kobayashi, C., & Nomoto, K. 2009, ApJ, 707, 1466
Kobayashi, C., Umeda, H., Nomoto, K., Tominaga, N., & Ohkubo, T. 2006, ApJ, 653, 1145
Koposov, S. E., Belokurov, V., Li, T. S., et al. 2019, MNRAS, 485, 4726
Koposov, S. E., Erkal, D., Li, T. S., et al. 2023, MNRAS, 521, 4936
Koposov, S. E., Rix, H.-W., & Hogg, D. W. 2010, ApJ, 712, 260
Laevens, B. P. M., Martin, N. F., Bernard, E. J., et al. 2015, ApJ, 813, 44
Law, D. R., & Majewski, S. R. 2010, ApJ, 714, 229
Li, G.-W., Yanny, B., Zhang, H.-T., et al. 2017, RAA, 17, 062
Li, T. S., Ji, A. P., Pace, A. B., et al. 2022, ApJ, 928, 30
Lianou, S., & Cole, A. A. 2013, A&A, 549, A47
Lilleengen, S., Petersen, M. S., Erkal, D., et al. 2023, MNRAS, 518, 774
Longeard, N., Martin, N., Ibata, R. A., et al. 2019, MNRAS, 490, 1498
Majewski, S. R., Skrutskie, M. F., Weinberg, M. D., & Ostheimer, J. C. 2003, ApJ, 599, 1082
Majewski, S. R., Schiavon, R. P., Frinchaboy, P. M., et al. 2017, AJ, 154, 94
Maoz, D., & Mannucci, F. 2012, PASA, 29, 447
Matsuno, T., Dodd, E., Koppelman, H. H., et al. 2022, A&A, 665, A46
Matteucci, F., & Recchi, S. 2001, ApJ, 558, 351
Mendelsohn, E. J., Newberg, H. J., Shelton, S., et al. 2022, ApJ, 926, 106
Mészáros, S., Martell, S. L., Shetrone, M., et al. 2015, AJ, 149, 153
Mészáros, S., Masseron, T., García-Hernández, D. A., et al. 2020, MNRAS, 492, 1641
Mucciarelli, A., Bellazzini, M., Ibata, R., et al. 2012, MNRAS, 426, 2889
Naidu, R. P., Conroy, C., Bonaca, A., et al. 2020, ApJ, 901, 48
Naidu, R. P., Conroy, C., Bonaca, A., et al. 2022, arXiv:2204.09057
Newberg, H. J., Willett, B. A., Yanny, B., & Xu, Y. 2010, ApJ, 711, 32
Nidever, D. L., Holtzman, J. A., Allende Prieto, C., et al. 2015, AJ, 150, 173
Nomoto, K., Kobayashi, C., & Tominaga, N. 2013, ARA&A, 51, 457
Odenkirchen, M., Grebel, E. K., Dehnen, W., et al. 2003, AJ, 126, 2385
Pancino, E., Romano, D., Tang, B., et al. 2017, A&A, 601, A112
Price-Whelan, A. M. 2017, JOSS, 2, 388
Price-Whelan, A. M., & Bonaca, A. 2018, ApJL, 863, L20
Samland, M. 1998, ApJ, 496, 155
Sanders, J. L., Belokurov, V., & Man, K. T. F. 2021, MNRAS, 506, 4321
Searle, L., & Zinn, R. 1978, ApJ, 225, 357
Sesar, B., Grillmair, C. J., Cohen, J. G., et al. 2013, ApJ, 776, 26
Shipp, N., Price-Whelan, A. M., Tavangar, K., Mateu, C., & Drlica-Wagner, A. 2020, AJ, 160, 244
Shipp, N., Drlica-Wagner, A., Balbinot, E., et al. 2018, ApJ, 862, 114
Shipp, N., Li, T. S., Pace, A. B., et al. 2019, ApJ, 885, 3
Smiljanic, R., Romano, D., Bragaglia, A., et al. 2016, A&A, 589, A115
Strigari, L. E., Bullock, J. S., Kaplinghat, M., et al. 2008, Natur, 454, 1096
Ting, Y.-S., Rix, H.-W., Conroy, C., Ho, A. Y. Q., & Lin, J. 2017, ApJL, 849, L9
Tolstoy, E., Hill, V., & Tosi, M. 2009, ARA&A, 47, 371
Villanova, S., Geisler, D., Carraro, G., Moni Bidin, C., & Muñoz, C. 2013, ApJ, 778, 186
Wilson, J. C., Hearty, F. R., Skrutskie, M. F., et al. 2019, PASP, 131, 055001
Yanny, B., Rockosi, C., Newberg, H. J., et al. 2009, AJ, 137, 4377
Zamora, O., García-Hernández, D. A., Allende Prieto, C., et al. 2015, AJ, 149, 181
Zasowski, G., Cohen, R. E., Chojnowski, S. D., et al. 2017, AJ, 154, 198